SCIENCE CHINA
Information Sciences

• LETTER •

August 2026, Vol. 69, Iss. 8, 180509:1–180509:2
https://doi.org/10.1007/s11432-026-5043-8

Special Topic: Quantum Information

Efficient self-consistent quantum comb tomography on the product Stiefel manifold

Xinlin HE[1,2†], Zetong LI[3†], Congcong ZHENG[1,2], Sixuan LI[1,2], Xutao YU[1,2*], Ling QIAN[4*], Runqing ZHANG[4], Zhiguo HUANG[4], Jize HAN[4] & Zaichen ZHANG[2,5*]

[1]*State Key Lab of Millimeter Waves, Southeast University, Nanjing 211189, China*
[2]*Frontiers Science Center for Mobile Information Communication and Security, Southeast University, Nanjing 210096, China*
[3]*Thrust of Artificial Intelligence, Information Hub, The Hong Kong University of Science and Technology (Guangzhou), Guangzhou 511453, China*
[4]*China Mobile (Suzhou) Software Technology Co., Ltd., Suzhou 215163, China*
[5]*National Mobile Communications Research Laboratory, Southeast University, Nanjing 210096, China*

Received 30 January 2026/Revised 21 May 2026/Accepted 13 July 2026/Published online 16 July 2026

Citation He X L, Li Z T, Zheng C C, et al. Efficient self-consistent quantum comb tomography on the product Stiefel manifold. Sci China Inf Sci, 2026, 69(8): 180509, https://doi.org/10.1007/s11432-026-5043-8

Quantum combs give a causal description of multi-time quantum processes with finite memory and provide a natural language for non-Markovian noise in quantum devices [1]. Existing quantum comb tomography (QCT) usually assumes that the inserted instruments and initial states are known exactly. This assumption is fragile on real hardware: imperfect instruments are absorbed into the reconstructed comb, so two imperfect instrument sets can give inconsistent estimates of the same process. Isometry-based QCT (iQCT) [2] reduces the computational cost of comb reconstruction through an isometric parametrization on the Stiefel manifold, yet it inherits the same known-instrument assumption and is therefore not self-consistent. Recent non-Markovian gate set tomography addresses self-consistency but still relies on Choi-state representations with large constrained parameter spaces [3]. We address both issues by reconstructing the comb, instruments, and initial states jointly on the product Stiefel manifold.

For an N-slot process, let $\mathcal{C}^{(N)}$ be the comb, $\mathfrak{J}^{(t)} = \{\mathcal{J}_v^{(t)}\}_v$ be the available instrument set at slot t, and $\mathfrak{S} = \{\rho_u^{(0)}\}_u$ be the initial-state set. The collection

$$\Gamma = \{\mathcal{C}^{(N)}, \mathfrak{J}^{(0)}, \ldots, \mathfrak{J}^{(N-1)}, \mathfrak{S}\}$$

is called a comb-instrument-state (CIS) set. For an instrument branch sequence $\mathcal{A}^{(0)}_{v_0,x_0}, \ldots, \mathcal{A}^{(N-1)}_{v_{N-1},x_{N-1}}$, the observed probability is

$$p^{(N)}_{\mathbf{x}_u,\mathbf{v}} = \mathrm{Tr}\Big[\mathcal{C}^{(N)}\left(\mathcal{A}^{(N-1)}_{v_{N-1},x_{N-1}} \circ \cdots \circ \mathcal{A}^{(0)}_{v_0,x_0}\right)\left(\rho_u^{(0)}\right)\Big]. \tag{1}$$

Optimizing a smooth objective $\mathcal{F}$ with respect to the CIS set amounts to solving the constrained problem

$$\min_{\Gamma} \ \mathcal{F}(\Gamma) \quad \text{s.t. Eqs. (3a)–(3d)}, \tag{2}$$

where the Choi operators are subject to physical feasibility:

$$\Upsilon^{(N)} \geqslant 0, \tag{3a}$$

$$\mathrm{Tr}_{\mathrm{o}_t} \Upsilon^{(t+1)} = I_{\mathrm{i}_t} \otimes \Upsilon^{(t)}, \quad \Upsilon^{(0)} = 1, \tag{3b}$$

$$A^{(t)}_{v,x} \geqslant 0, \quad \sum_x \mathrm{Tr}_{\mathrm{i}_{t+1}} A^{(t)}_{v,x} = I_{\mathrm{o}_t}, \tag{3c}$$

$$\rho_u^{(0)} \geqslant 0, \quad \mathrm{Tr}\,\rho_u^{(0)} = 1. \tag{3d}$$

Here Eq. (3a) enforces complete positivity of the comb, Eq. (3b) enforces causality, Eq. (3c) enforces complete positivity and trace preservation for each complete instrument, and Eq. (3d) enforces state normalization. Solving Eq. (2) directly is intractable, and bounded memory further imposes rank constraints on the Choi operators.

Theorem 1. For every admissible CIS set Γ, choose ancillary dimensions $d_{a_{t+1}} \geqslant \mathrm{rank}(\Upsilon^{(t+1)})$, $d_{e_{t,v,x}} \geqslant \mathrm{rank}(A^{(t)}_{v,x})$, and $d_{r_u} \geqslant \mathrm{rank}(\rho_u^{(0)})$. Then Γ admits a parametrization by isometries $\Gamma = \Gamma(\mathbb{V}, \mathbb{J}, \mathbb{S})$ on the product Stiefel manifold

$$\mathcal{M} = \Big[\bigtimes_{t=0}^{N-1} \mathrm{St}(d_{\mathrm{o}_t} d_{a_{t+1}}, d_{\mathrm{i}_t} d_{a_t})\Big] \times \left[\bigtimes_{t,v} \mathrm{St}\left(\sum_x d_{\mathrm{i}_{t+1}} d_{e_{t,v,x}}, d_{\mathrm{o}_t}\right)\right] \times \Big[\bigtimes_u \mathrm{St}(d_{\mathrm{i}_0} d_{r_u}, 1)\Big],$$

where $V^{(t)} : \mathcal{H}_{\mathrm{i}_t} \otimes \mathcal{H}_{a_t} \to \mathcal{H}_{\mathrm{o}_t} \otimes \mathcal{H}_{a_{t+1}}$ carries the memory ancilla $\mathcal{H}_{a_t}$, $J_v^{(t)} = [W^{(t)}_{v,1}, \ldots, W^{(t)}_{v,|\mathcal{J}_v^{(t)}|}]^{\mathrm{T}}$ stacks the branches of the v-th instrument at slot t, and S_u is a purification of $\rho_u^{(0)}$. Conversely, every point on $\mathcal{M}$ induces a physically valid CIS representative satisfying complete positivity, causality, trace preservation of each complete instrument, and state normalization.

The comb part follows from the isometry cascade of causal quantum combs [4], with $\mathcal{H}_{a_t}$ the memory ancilla carrying system-environment correlations across slots. The instrument part follows

* Corresponding author (email: yuxutao@seu.edu.cn, qianling@cmss.chinamobile.com, zczhang@seu.edu.cn)
† These authors contributed equally to this work.

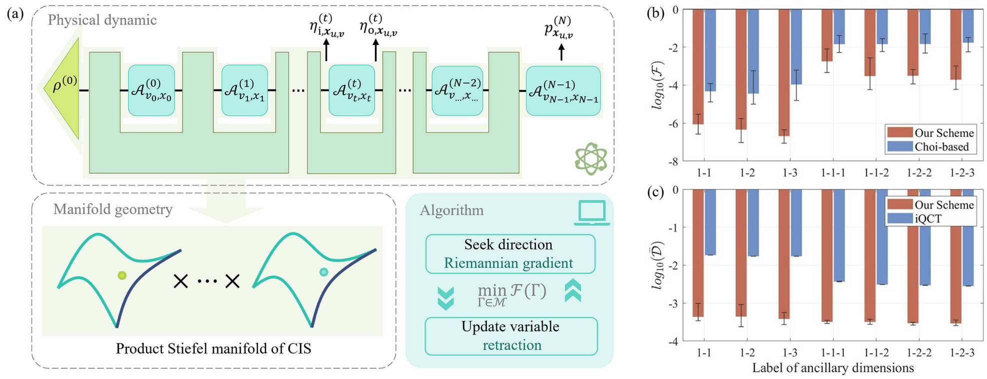

Figure 1 (Color online) Framework and validation. (a) General framework. A CIS set is reconstructed by Riemannian optimization algorithm on the product Stiefel manifold, turning physically constrained reconstruction into unconstrained manifold optimization. (b) Numerical simulation versus a full dense Choi-state self-consistent baseline: reconstruction loss (log scale; means over 10 trials, error bars span $[\min, \max]$). (c) Hardware experiment on Wuyue-1 versus iQCT: average squared probability distance $\bar{\mathcal{D}}$ (10 repetitions).

from Stinespring dilation of each branch, and the state part from purification. Theorem 1 turns the constrained problem (2) into unconstrained Riemannian optimization on $\mathcal{M}$. The parametrization is not injective: auxiliary-space and system-space gauge transformations leave all observable probabilities invariant, so reconstructions are interpreted up to gauge equivalence.

Figure 1(a) summarizes the workflow. Experiments enumerate initial-state labels and instrument sequences, and repeated shots estimate the empirical probabilities $\tilde{p}^{(t)}_{\mathbf{x}_{u,\mathbf{v}}}$. The reconstruction minimizes

$$\min_{(\mathbb{V},\mathbb{J},\mathbb{S})\in\mathcal{M}} \sum_{t} \sum_{\mathbf{x}_{u,\mathbf{v}}} \left(\tilde{p}^{(t)}_{\mathbf{x}_{u,\mathbf{v}}} - p^{(t)}_{\mathbf{x}_{u,\mathbf{v}}}\right)^2, \tag{4}$$

where $\mathcal{M}$ denotes the product Stiefel manifold. Under this representation, all observable statistics are determined by the CIS configuration up to gauge equivalence. In standard QCT, the probabilities depend linearly on the comb Choi operator and informational completeness reduces to a linear-injectivity requirement. In the self-consistent formulation, the probabilities become a nonlinear function of $(\mathbb{V},\mathbb{J},\mathbb{S})$: the spanning condition serves only as a probing-design criterion ensuring operator-space coverage at each slot, and does not by itself constitute a complete identifiability theorem, since gauge-equivalent configurations remain indistinguishable. The recursive probability evaluation is

$$\eta^{(t)}_{\mathrm{i}} = V^{(t)} \eta^{(t-1)}_{\mathrm{o}} V^{(t)\dagger}, \tag{5}$$

$$\eta^{(t)}_{\mathrm{o}} = \mathrm{Tr}_{e_t,v,x}\left[W^{(t)}_{v,x} \eta^{(t)}_{\mathrm{i}} W^{(t)\dagger}_{v,x}\right], \tag{6}$$

with $\eta^{(-1)}_{\mathrm{o}} = \rho^{(0)}_u$ and $p^{(t)}_{\mathbf{x}_{u,\mathbf{v}}} = \mathrm{Tr}[\eta^{(t)}_{\mathrm{o}}]$. Here $\eta^{(t)}_{\mathrm{i}}$ and $\eta^{(t)}_{\mathrm{o}}$ are the input and output states of the slot-t instrument branch: the comb link acts first and the instrument acts afterward. We optimize (4) by Riemannian ADAM, using tangent-space gradients and retractions on the Stiefel factors [5].

The per-iteration complexity of complex multiplication of our method is $\mathcal{O}(|\mathfrak{S}| n_A^N m^N d^3 d_e \sum_{t=0}^{N-1} d^3_{a_{t+1}})$, while the dense Choi-based baseline has the complexity $\Omega(|\mathfrak{S}| n_A^N m^N d^{4N})$. Thus the advantage is most pronounced for bounded-memory combs, where the ancillary dimensions are small compared with the full Choi dimension.

We implemented the method in C++ and tested it on both simulated and hardware data. In numerical tests, overcomplete CPTNI instruments and randomized non-Markovian combs were used to generate data. Compared with a full dense Choi-state self-consistent baseline, the product Stiefel method reached lower reconstruction loss $\mathcal{F}$ across the tested ancillary dimensions (Figure 1(b)); the label "$\log_2 d_{a_1}$-$\log_2 d_{a_2}$" denotes $\log_2$ of the ancillary dimensions at consecutive time steps, and bars are means over 10 trials with error bars spanning $[\min, \max]$. Because the simulated comb, instruments, and initial states are known, the synthetic tests also exhibit improved physical reconstruction after gauge alignment.

Hardware experiments were performed on the Wuyue-1 superconducting processor. The deployed single-qubit instruments included calibrated CPTP operations and Pauli-basis measurement operations. On the hardware data, our method attains a smaller average squared probability distance $\bar{\mathcal{D}} = \mathcal{F}/N_p$ (with N_p the number of terms) than iQCT, which assumes known instruments and states, across all tested ancillary dimensions (Figure 1(c)). Since no ground-truth comb is available on the device, the comb fidelity between our estimate and the iQCT estimate is reported only as a consistency comparison with the iQCT reference, not as an absolute reconstruction-fidelity metric.

As a result, both the numerical and hardware experiments indicate reliable recovery of the CIS set under realistic noise. However, this should not be conflated with a proof of identifiability since the CIS set exhibits gauge equivalence. The informational completeness to uniquely estimate a CIS set remains an open problem. These results demonstrate that our method provides a practical route for characterizing non-Markovian processes with reduced computational overhead.

Acknowledgements This work was supported by National Natural Science Foundation of China (Grant No. 62471126), Frontier Technologies R&D Program of Jiangsu (Grant No. BF2025066), Jiangsu Key R&D Program Project (Grant No. BE2023011-2), and Fundamental Research Funds for the Central Universities (Grant No. 2242022k60001).

Supporting information The supporting information is available online at info.scichina.com and link.springer.com. The supporting materials are published as submitted, without typesetting or editing. The responsibility for scientific accuracy and content remains entirely with the authors.

References

1 Pollock F A, Rodríguez-Rosario C, Frauenheim T, et al. Non-Markovian quantum processes: complete framework and efficient characterization. Phys Rev A, 2018, 97: 012127
2 Li Z T, He X L, Zheng C C, et al. Quantum comb tomography via learning isometries on stiefel manifold. Phys Rev Lett, 2025, 134: 010803
3 Li Z T, Zheng C C, Meng F X, et al. Non-Markovian quantum gate set tomography. Quantum Sci Technol, 2024, 9: 035027
4 Bisio A, D'Ariano G M, Perinotti P, et al. Minimal computational-space implementation of multiround quantum protocols. Phys Rev A, 2011, 83: 022325
5 Boumal N. An Introduction to Optimization on Smooth Manifolds. Cambridge: Cambridge University Press, 2023